Received: 14 May 2019 | Revised: 5 September 2019 | Accepted: 29 November 2019 | Published on: 8 January 2020

DOI: 10.1002/met.1880

RESEARCH ARTICLE

Meteorological Applications RMetS

On stability correction functions over the Indian region under stable conditions

Piyush Srivastava[1,2] | **Maithili Sharan**[1] | **Manoj Kumar**[3] | **Aditya Kumar Dhuria**[1]

[1]Centre for Atmospheric Sciences, Indian Institute of Technology Delhi, Delhi, India

[2]School of Earth and Environment, University of Leeds, Leeds, UK

[3]School of Natural Resource Management, Center for Environmental Sciences, Central University of Jharkhand, Ranchi, Jharkhand, India

Correspondence
Maithili Sharan, Centre for Atmospheric Sciences, Indian Institute of Technology Delhi, Hauz Khas, Delhi-110016, India.
Email: mathilis@cas.iitd.ac.in

Funding information
DST, Science and Engineering Research Board (SERB), Grant/Award Number: SB/S2/JCB-79/2014

Abstract

Turbulence observations over an Indian region are used to examine the observational behaviour of stability-correction functions for momentum (φ_m) and heat (φ_h) under stable conditions within the framework of Monin–Obukhov similarity theory. The φ_m is observed to follow the linear functional form in the case of near-neutral to moderately stable conditions. However, φ_m is found to increase with a relatively slower rate as compared with the linear form in strongly stable conditions. A large scatter in φ_h is observed with the near-neutral condition, and they tend to level off in very stable conditions. The optimized co-efficients appearing in the functional form of φ_m suggested by Grachev *et al*. in 2007 are derived using turbulence observations. The present study recommends the use of these optimized functional forms of φ_m and φ_h for the estimation of surface fluxes over an Indian region in atmospheric models.

KEYWORDS

atmospheric surface layer, Monin–Obukhov similarity theory, similarity functions, stable conditions, turbulence data

1 | INTRODUCTION

The lowest part of the atmospheric boundary layer, wherein the surface fluxes vary by < 10% of their magnitude, is known as an atmospheric surface layer (ASL) (Stull, 1988). The parameterization of the surface layer turbulent fluxes is required in atmospheric weather and climate models. The Monin–Obukhov similarity theory (MOST; Monin and Obukhov, 1954) is normally applied to parameterize the surface fluxes in the atmospheric models (Arya, 1988; Garratt, 1994; Mahrt, 1998; Skamarock *et al*., 2008; Jimenez *et al*., 2012; Pielke, 2013; Zhang *et al*., 2015). The dimensionless stability-correction functions for wind and temperature, φ_m and φ_h, respectively, are the key parameters in the estimation of surface fluxes in atmospheric models. According to the MOST, φ_m and φ_h are universal functions of Monin–Obukhov stability parameter ζ. However, the theory does not provide the exact functional form of these functions, except certain asymptotic predictions in the case of near-neutral and very stable/unstable conditions. Various functional forms of these functions have been developed over the years by analysing the turbulence measurements over different sites in various atmospheric conditions while keeping the theoretical asymptotic limit imposed by the MOST as primary constraints on the nature of these

functions (Grachev *et al.*, 2007a). However, the applicability of these "site-specific" empirical functional forms in different stability regimes is still debatable (Grachev *et al.*, 2007a; Luhar *et al.*, 2009; Srivastava and Sharan, 2019). Furthermore, these empirical stability-correction functions are not systematically evaluated over the Indian subcontinent. In order to validate the parameterization schemes and possible modification over the Indian subcontinent, several field experiments were carried out. Data acquired from the field experiments over the Indian subcontinent and various other independent micrometeorological towers installed at different sites were used periodically in order to study the turbulent characteristics over the subcontinent (Ramachandran *et al.*, 1994; Rao *et al.*, 1996; Krishnan and Kunhikrishnan, 2002; Ramana *et al.*, 2004; Rao and Narasimha, 2006; Patil, 2006; Aditi and Sharan, 2007; Bhat and Narasimha, 2007; Tyagi *et al.*, 2012; Srivastava and Sharan, 2015; Reddy and Rao, 2016; Sharan and Srivastava, 2016; Rao and Reddy, 2019). This has led to the improved understanding of boundary/surface layer features over land as well as ocean surfaces. However, to the present authors' knowledge, no attempt has been made to analyse the functional behaviour of the stability-correction functions over the Indian region. It is generally assumed that the MOST, if it works, removes the dependency on geographical location or subregion. Consequently, various MOST-based functional forms such as normalized turbulence quantities and the stability-correction functions should exhibit a universal behaviour independent of the regional features of the measurement site. However, owing to the empirical nature of the stability-correction functions and complex physical phenomenon occurring in the weak wind-stable boundary layer, there is still a need to evaluate the existing functional forms of these functions for application in numerical models. Further, some of the recent studies have questioned the applicability of existing stability-correction functions in a theoretical framework (Sharan and Kumar, 2011; Srivastava and Sharan, 2019). Sharan and Kumar (2011) have pointed out the unphysical non-monotonic nature of drag co-efficient in the stable boundary layer predicted by various nonlinear stability-correction functions and deduced a limit of applicability of these empirical functions in a theoretical framework. Recently, Srivastava and Sharan (2019) have pointed out the inconsistency of the various functional forms of φ_m in the light of the occurrence of unusual second maxima in the heat flux and stability relationship, which originates from a too quick levelling off of the function φ_m. They argued that the functional forms of φ_m should be revised to make the secondary peak appearing in the heat flux and stability relationship less pronounced. Based on the findings of Srivastava and Sharan, an attempt is made in the present paper to analyse the observed functional behaviour of the stability-correction functions to make them consistent for use in the estimation of surface fluxes over an Indian region.

2 | FORMAL BACKGROUND

According to the MOST, in a homogeneous and stationary surface layer, the gradients of mean wind speed and virtual potential temperature profiles behave as:

$$\frac{kz}{u_*}\frac{\partial U}{\partial z} = \varphi_m(\zeta) \tag{1}$$

$$\frac{kz}{\theta_*}\frac{\partial \theta_v}{\partial z} = \varphi_h(\zeta), \tag{2}$$

where k is the von Karman constant; z is the height above the ground; u_* and θ_* are, respectively, friction velocity and the temperature scales; and φ_m and φ_h are, respectively, the non-dimensional similarity functions. U and θ_v, respectively, represent wind speed and temperature at measurement level z. The Monin–Obukhov stability parameter ζ is defined as:

$$\zeta = \frac{kzg}{\bar{\theta_v}}\frac{\theta_*}{u_*^2} \tag{3}$$

where $\bar{\theta_v}$ is the mean virtual temperature (K).

The functions φ_m and φ_h have the form:

$$\varphi_m(\zeta) = (1 + \beta_m\zeta) \tag{4}$$

$$\varphi_h(\zeta) = Pr_t(1 + \beta_h\zeta), \tag{5}$$

where β_m and β_h are constants; and Pr_t is the turbulent Prandtl number indicating the dissimilarity between the turbulent transfer of momentum and sensible heat (Grachev *et al.*, 2007a; Li, 2019). In other words, the turbulent Prandtl number also describes a ratio between the stability-correction functions of heat and momentum as $\mathrm{Pr}_t = \varphi_h/\varphi_m$. The dependency of the turbulent Prandtl number on the extent of stability of the stable atmosphere is still a point of uncertainty. The contradictory nature of Pr_t with stability has been reported in several studies depending upon the parameter, which is being used to quantify the extent of stability of the ASL and amount of self-correlation (Grachev *et al.*, 2007b). The commonly used stability parameters are the Monin–Obukhov stability parameter ζ, the gradient Richardson number Ri, the flux Richardson number Ri_f and the bulk Richardson number Ri_B. From the analysis of the Surface Heat Budget of the Arctic Ocean (SHEBA)

experiment data set, Grachev *et al.* (2007b) argued that Pr_t decreases with increasing stability and it remains < 1 in very stable conditions, provided that Ri_B is used to classify the stability of the atmospheric boundary layer. For other stability parameters, the Pr_t shows contradictory behaviour due to self-correlation (Grachev *et al.*, 2007b). The linear functional form (Equations 4 and 5) can also be treated as a blending between the two extreme stability conditions: (a) neutral stability in which $\varphi_m = \varphi_h = 1$; and (b) very stable conditions in which turbulence does not effectively communicate with the underlying surface and the height above the surface becomes an insignificant scaling parameter (Grachev *et al.*, 2013), leading to the expression $\varphi_{m,\,h} = \beta_{m,\,h}\zeta$. The concept that height above the surface is not a relevant scaling parameter for the MOST relationship in very stable conditions is termed a local z-less scaling concept (Wyngaard, 2010; Grachev *et al.*, 2013). The validity of these linear functions in ζ is limited to $\zeta \leq \zeta_c$, where ζ_c is usually taken as being of the order of 1. To overcome the limitation of linear functional forms of the similarity functions, various nonlinear expressions for φ_m and φ_h have been proposed by researchers over the years (Clarke, 1970; Hicks, 1976; Holtslag and De Bruin, 1988; Beljaars and Holtslag, 1991; Cheng and Brutsaert, 2005; Grachev *et al.*, 2007a). Those can be used for the computation of surface fluxes under near-neutral to very stable conditions. Sharan and Kumar (2011) have pointed out that the functions suggested by Holtslag and De Bruin (1988), Cheng and Brutsaert (2005), and Grachev *et al.* (2007a) are "theoretically" valid for the entire range of stability. Recently, the stability-correction functions suggested by Cheng and Brutsaert (2005) are introduced in the fifth-generation Pennsylvania State University–National Center for Atmospheric Research Mesoscale Model (MM5) parameterization (Grell, Dudhia, Stauffer, 1994) to parameterize surface fluxes under stable conditions in the Weather Research and Forecast (WRF) model while those suggested by Grachev *et al.* (2007a) are being used in the boundary layer studies over the Arctic region (Gryanik and Lupkes, 2018).

3 | A BRIEF DESCRIPTION OF SITE AND DATA SET

This section describes the data set and estimates the turbulence quantities in parallel to that of Sharan and Srivastava (2016) and Srivastava and Sharan (2019).

Data from a fast-response sensor (CSAT3 Sonic anemometer) installed at 10 m height at the Birla Institute of Technology Mesra in Ranchi (23.412° N, 85.440° E), India, with an average elevation 609 masl (http://odis.incois.gov.in/index.php/project-datasets/ctcz-programme/data) (Dwivedi *et al.*, 2014) are used. Turbulence measurements at 10 Hz frequency for 2009 are used to calculate the hourly fluxes using the eddy covariance technique (Srivastava and Sharan, 2015; Sharan and Srivastava, 2016). Friction velocity u_* is calculated using:

$$u_* = \left[\left(\overline{u'w'}\right)^2 + \left(\overline{v'w'}\right)^2\right]^{1/4}, \tag{6}$$

where u', v' and w' are, respectively, the fluctuations in longitudinal, lateral and vertical wind components. The stability parameter ζ is calculated from Equation 3.

The slow measurements (1 Hz) of multilevel wind and temperature observations are used to evaluate the vertical wind and temperature gradients (Equations 1 and 2). These gradients are obtained by fitting the following second-order polynomials through a 1 hr profile similar to Grachev *et al.* (2005) and Srivastava and Sharan (2019):

$$U(z) = a_0 + a_1(\ln z) + a_2(\ln z)^2 \tag{7}$$

$$\theta_v(z) = b_0 + b_1(\ln z) + b_2(\ln z)^2, \tag{8}$$

where $U(z)$ and $\theta_v(z)$, respectively, are the wind speed and temperature at measurement level z. The hourly averaged wind and temperature observations obtained at 1, 2, 4, 8, 16 and 32 m heights are used to evaluate the unknown co-efficients $a_i s$ and $b_i s$ using a classical least-squares approach; the hourly wind and temperature gradients are then estimated. Notice that in the current formulations, the mean wind defined by Equation 7 does not satisfy the "no-slip" condition at the ground surface. Similarly, the virtual potential temperature in Equation 8 does not retrieve the surface temperature at the ground surface. Thus, instead of fitting these mean variables as a function of z only, one can fit the multilevel wind and temperature observations as functions of dimensionless heights z/z_0 and z/z_h, where z_0 and z_h are, respectively, aerodynamic and thermal roughness lengths. However, this requires the estimation of roughness lengths of heat and momentum. The estimation of the roughness length of heat would require the surface temperature, which is not available for the current measurement site. Further, large variability in the roughness lengths would introduce even more uncertainty in the estimated gradients.

The gradient and flux Richardson numbers are derived, respectively, using:

$$Ri = \frac{g}{\overline{\theta}_v} \frac{\partial\theta_v/\partial z}{\left(\partial U/\partial z\right)^2} \tag{9}$$

$$Ri_f = -\left(\frac{g}{\bar{\theta}_v}\right)\frac{\left(w'\bar{\theta}_v'\right)}{u_*^2(\partial U/\partial z)}, \quad (10)$$

The correction functions φ_m and φ_h are calculated using Expressions (1) and (2). The flux Richardson number is the ratio of the buoyancy term to the shear term of the turbulent kinetic energy (TKE) budget equation. The TKE budget equation suggests that for continuous turbulence, the flux Richardson number should be < 1. For the data presented here, there is a significant amount of data points for which $Ri_f > 1$ (Figure 1). Luhar *et al.* (2009) have argued that $Ri_f > 1$ is generally associated with the non-homogenous or unsteady state conditions in which the MOST is inapplicable. Grachev *et al.* (2013) have suggested that the local MOST is applicable only in the regime for which both the gradient and flux Richardson numbers are less than the critical value 0.25. Based on the approach of Grachev *et al.* (2013) and used by Srivastava and Sharan (2019), the present study considers two subsets of data: (1) filtered data for which the gradient and flux Richardson numbers are < 0.25; and (1) the whole data set. For the filtered data set, $\zeta < 1.5$ (Figure 1a), while for the whole data, very large ζ, reaching an approximate order of hundreds (Figure 1b).

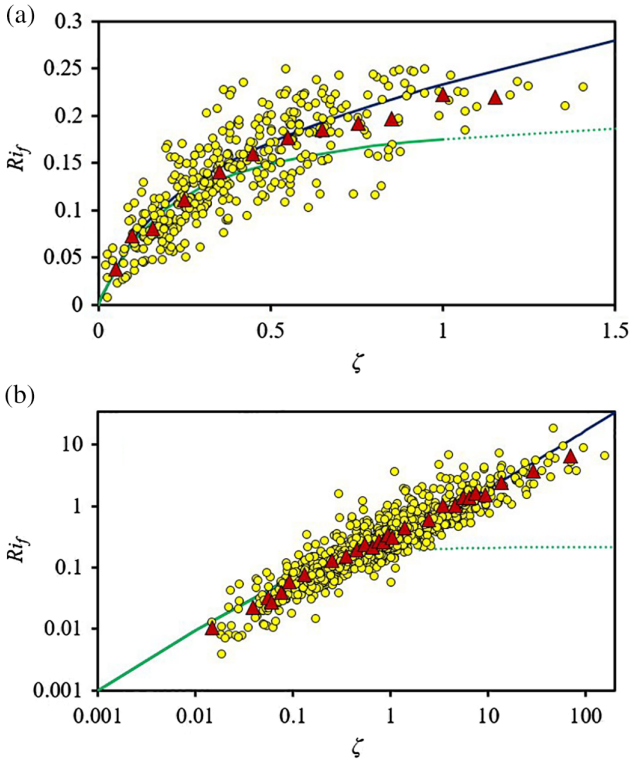

FIGURE 1 Variation of flux Richardson number Ri_f with stability parameter ζ for (a) filtered data and (b) whole data. The corresponding bin-averaged data are shown with red triangles. The green line represents the theoretical $Ri_f = \zeta/\varphi_m$ for linear similarity function $\varphi_m = 1 + \beta_m\zeta$ (Businger *et al.*, 1971). The dotted green line represents the corresponding values in an extended range of φ_m beyond the range of applicability of linear form, that is, $\zeta \leq 1$. The dark blue line shows the Ri_f obtained using the functional form of φ_m suggested by Grachev *et al.* (2007a)

4 | FLUX-PROFILE RELATIONSHIP

The section discusses first the observed variation of φ_m, followed by the analysis of observed nature of φ_h with stability parameter ζ for the filtered data set. Further, the observed nature of both φ_m and φ_h will be analysed for the whole data set without imposing the prerequisite on the flux and gradient Richardson numbers. Since the φ_m, φ_h and ζ cover a wide range of values, logarithmic axes are chosen in some of the graphs for a better representation of the results.

Figure 2 shows the stability function of momentum (φ_m) plotted *versus* the Monin–Obukhov stability parameter ζ for Ranchi for the filtered data set. The averages of φ_m are computed in equally spaced stability bins within each decade in the stability, which is shown with red triangles. The linear similarity function $\varphi_m = 1 + \beta_m\zeta$ with $\beta_m = 4.7$ (Businger *et al.*, 1971) is drawn with a green line, while the dotted green line represents the linear function in an extended range beyond the range of its applicability, that is, $\zeta \leq 1$. The functional form suggested by Cheng and Brutsaert (2005) based on CASES-99 data is plotted with a red line for comparison. Figure 2a suggests that in near-neutral to moderately stable conditions ($0 < \zeta < 0.5$), the φ_m increases with increasing stability following the classical linear functional form and Cheng and Brutsaert (2005) functional form with a similar slope. However, from moderately to strongly stable conditions ($0.5 < \zeta < 2.0$), the φ_m increases with a relatively slower rate as compared with that predicted by the linear functional form. Based on the analysis of field data over various sites, a wide range of β_m have been reported in the literature. For example, Brutsaert (1982) has recommended $\beta_m = 5$; Foken (2006) has documented that $\beta_m = 6$ is generally used for operational purposes. All the other larger β_m support the present argument that φ_m is observed to increase with a relatively slower rate as compared with that predicted by linear functional form for $\zeta > 0.5$. The observed φ_m are relatively small as compared with that shown by the functional form suggested by Cheng and Brutsaert (2005) in the range $0.5 < \zeta < 2.0$. Figure 2b shows the variation of φ_m with ζ for the whole data. As expected, a relatively large scatter in φ_m is found to occur as compared with that obtained for the filtered data set. The φ_m are observed to increase with increasing

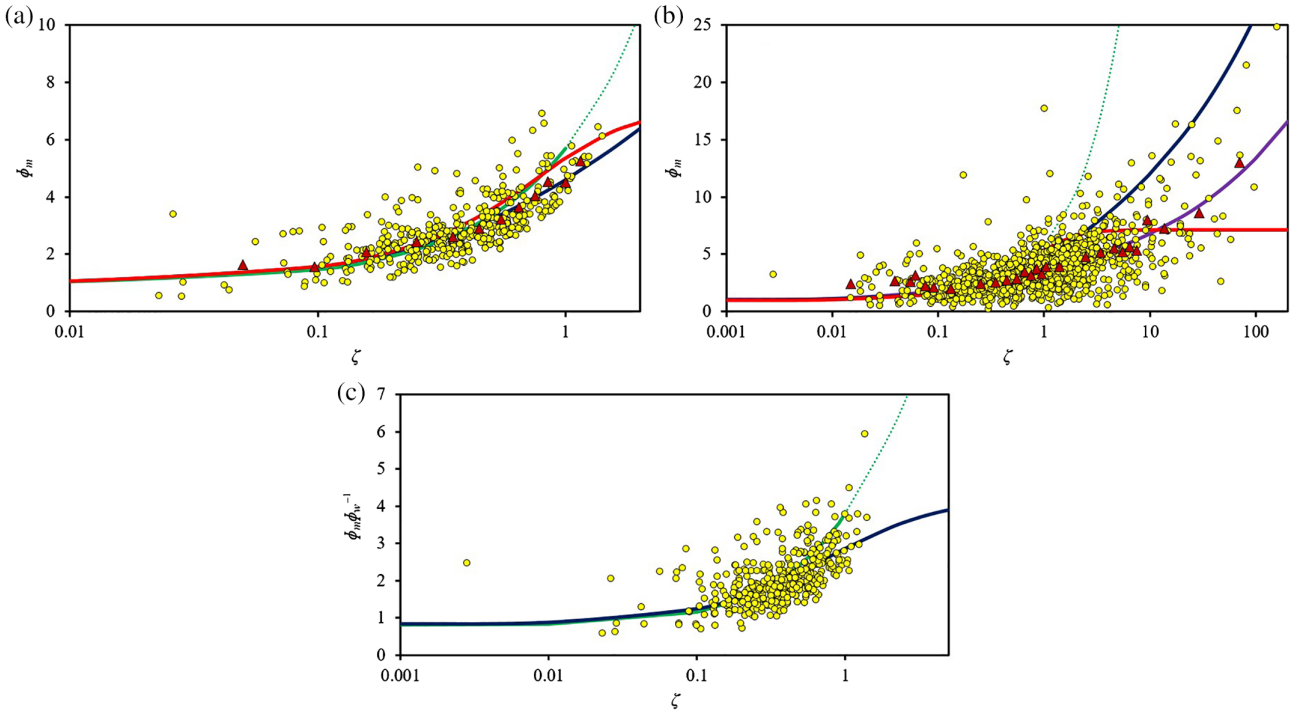

FIGURE 2 (a) Non-dimensional vertical gradients of mean wind speed φ_m plotted *versus* the Monin–Obukhov stability parameter ζ for Ranchi (India) for the filtered data set. The corresponding bin-averaged data are shown with red triangles. The green line represents a linear similarity function $\varphi_m = 1 + \beta_m\zeta$ (Businger *et al*., 1971). The dotted green line represents the linear function in an extended range beyond the range of its applicability, that is, $\zeta \leq 1$. The dark blue line is the best-fit curve obtained using the functional form suggested by Grachev *et al*. (2007a) with modified unknown co-efficients. The red line represents the functional form suggested by Cheng and Brutsaert (2005) based on CASES-99 data. (b) Non-dimensional vertical gradients of mean wind speed φ_m plotted *versus* the Monin–Obukhov stability parameter ζ for Ranchi for the whole data. The corresponding bin-averaged data are shown with red triangles. The green line represents a linear similarity function $\varphi_m = 1 + \beta_m\zeta$ (Businger *et al*., 1971). The dotted green line represents the linear function in an extended range beyond the range of its applicability, that is, $\zeta \leq 1$. The dark blue line represents the best-fit curve obtained for filtered data as in (a). The violet line is the best-fit curve obtained for the whole data. The red line represents the functional form suggested by Cheng and Brutsaert (2005) based on CASES-99 data. (c) As for (a), but for a combination of universal functions φ_m and φ_w as $\varphi_m\varphi_w^{-1} = \left(\frac{kz}{\sigma_w}\right)\frac{\partial U}{\partial z}$, which is not affected by the self-correlation. The dotted green line represents the ratio of $\varphi_m = 1 + \beta_m\zeta$ (Businger *et al*., 1971) and $\varphi_w = 1.25(1 + 0.2\zeta)$ (Kaimal and Finnigan, 1994). The dark blue line represents the ratio of $\varphi_m(\zeta) = 1 + \frac{5.4\zeta(1+\zeta)^{\frac{1}{3}}}{1+0.89\zeta}$, (Grachev *et al*., 2007a, with optimized co-efficients) and $\varphi_w = 1.21(1 + 1.34\zeta)^{1/3}$ (the best-fit curve for the present filtered data set)

stability at a relatively slower rate as compared with that suggested by the filtered data set. Note that the slow varying nature of φ_m is a well-documented fact (Webb, 1970; Holtslag and De Bruin, 1988; Beljaars and Holtslag, 1991). Based on the analysis of the famous CASES-99 data, Cheng and Brutsaert (2005) noted the slow increasing nature of φ_m with stability for $\zeta > 1$ and they developed new functional forms of φ_m and φ_h. In fact, this nature is discussed in detail by Srivastava and Sharan (2019). Almost all the earlier studies agree with the prediction of the linear functional form for small ζ. However, most of the earlier observations have pointed out a "level-off" characteristic for φ_m at higher stability (Webb, 1970; Cheng and Brutsaert, 2005), which suggests that φ_m becomes asymptotically constant at higher stability (Figure 2b). The assumption of Webb (1970) regarding a zero slope for $\zeta > 1$ results in a constant φ_m for $\zeta > 1$. Cheng and Brutsaert (2005) have also pointed out that φ_m asymptotically attains a constant value. This "level-off" nature leads to a "complete departure" of φ_m's function from the prediction of linear functional form suggested by Businger *et al*. (1971) in an extended range of ζ.

Recently, Srivastava and Sharan (2019) have argued that the functional form of φ_m suggested by Grachev *et al*. (2007a) is relatively more appropriate and consistent for application in numerical models. The functional form of φ_m is given by:

$$\varphi_m(\zeta) = 1 + \frac{a_m\zeta(1+\zeta)^{\frac{1}{3}}}{1 + b_m\zeta}. \tag{11}$$

where the co-efficients a_m and b_m take $a_m = 5$ and $b_m = a_m/6.5$. To develop an observation-based functional

form of the φ_m function, the functional form suggested by Grachev *et al.* was adopted and the optimal unknown co-efficients a_m and b_m were estimated for the data taken in the present study. These are $a_m = 5.4$ and $b_m = 0.89$ for the filtered data set. In Figure 2, the dark blue line represents the functional form suggested by Grachev *et al.* (Equation 11) with these optimal unknown co-efficients. This curve shows good agreement with the individual as well as the bin-averaged observational data. The updated φ_m function has a relatively smaller slope as compared with that shown by the linear form of φ_m function in strongly stable conditions. However, in the case of the whole data set in which no prerequisites for flux and gradient Richardson number are applied, both the linear as well as a functional form of φ_m derived from the filtered data are found to overestimate φ_m (Figure 2b). In such a condition, the optimal co-efficients appearing in the functional form of Grachev *et al.* (Equation 11) are $a_m = 2.67$ and $b_m = 0.27$, and the curve obtained with these modified co-efficients shows good agreement with the observational data (Figure 2b). However, the functional form of φ_m with these co-efficients does not satisfy the condition proposed by Srivastava and Sharan (2019), which is required for a consistent relationship between heat flux and stability parameter within the framework of the MOST. This is associated with the fact that φ_m's are observed to increase with ζ at a very slow rate. Note that the critical Ri_f is close to 0.25 for continuous turbulence and larger Ri_f's are generally associated with the weak and intermittent turbulence (Beljaars and Holtslag, 1991). Grachev *et al.* (2013) found the collapse of the inertial subrange for $Ri_f > 0.25$ with the existence of some small-scale turbulence. Thus, an extremely slower rate of increase as well as the levelling-off characteristic of the φ_m function with ζ, as observed in the present data set and earlier studies, is associated with the regime in which the MOST is not applicable in its present form. Figure 3a shows the stability functions of heat φ_h plotted *versus* ζ for the filtered data set. Similar to Figure 2a, the bin-averaged data are shown with red

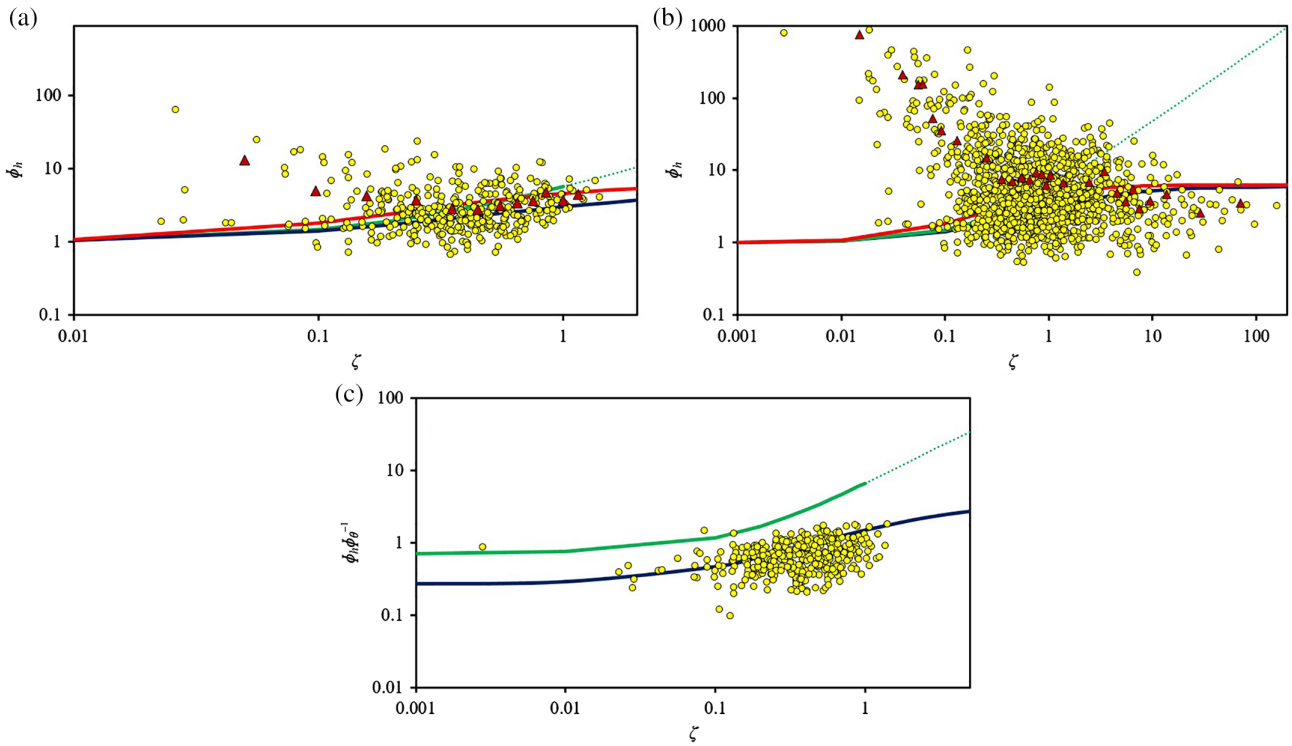

FIGURE 3 (a) Non-dimensional vertical gradients of mean temperature φ_h plotted *versus* the Monin–Obukhov stability parameter ζ for Ranchi (India) for the filtered data set. The corresponding bin-averaged data are shown with red triangles. The green line represents a linear similarity function $\varphi_h = 1 + \beta_h\zeta$ (Businger *et al.*, 1971). The dotted green line represents the linear function in an extended range beyond the range of its applicability, that is, $\zeta \leq 1$. The dark blue line is the best-fit curve obtained using the functional form suggested by Grachev *et al.* (2007a). The red line represents the functional form suggested by Cheng and Brutsaert (2005) based on CASES-99 data. (b) As for (a), but for whole data. (c) As for (a), but for a combination of universal functions φ_h and φ_θ as $\varphi_h\varphi_\theta^{-1} = \left(\frac{kz}{\sigma_\theta}\right)\frac{\partial\theta}{\partial z}$, which is not affected by the self-correlation. The dotted green line represents the ratio of $\varphi_h = 1 + \beta_h\zeta$ (Businger *et al.*, 1971) and $\varphi_\theta = 2.0(1 + 0.5\zeta)^{-1}$ (Kaimal and Finnigan, 1994). The dotted red line represents the ratio of $\varphi_h(\zeta) = 1 + \frac{5\zeta + 5\zeta^2}{1 + 3\zeta + \zeta^2}$, (Grachev *et al.*, 2007a, with optimized co-efficients) and $\varphi_\theta = 18.0(1 + 28.1\zeta)^{-0.5}$ (fitted curve for present filtered data set)

triangles. The linear form of the φ_h function is represented by a green line. The dotted green line represents the linear function in an extended range beyond the range of its applicability, that is, $\zeta \leq 1$. The dark blue line is the curve obtained using the functional form suggested by Grachev *et al.* (2007a). The red line represents the functional form suggested by Cheng and Brutsaert (2005). The φ_h's show a relatively large scatter than those obtained for φ_m. The unexpectedly large φ_h along with a large scatter in the near-neutral conditions have also been reported in earlier studies (Yagüe *et al.*, 2006; Grachev *et al.*, 2007a; Park *et al.*, 2009). Yagüe *et al.* (2006) have pointed out that the scatter in φ_h may be associated with the fact that the potential temperature gradient can be very small in the near-neutral conditions, leading to larger errors in the estimation of φ_h. The deviations in φ_h are found to be very large in the case of near-neutral to moderately stable conditions, and it is hard to predict a functional dependence of φ_h on stability. There is a relatively less scatter in φ_h for $\zeta > 0.5$ and it shows a levelling-off characteristic at a relatively higher ζ- (Figure 3a). The φ_h's show an even more larger scatter with ζ for the whole data set as compared with the filtered data set (Figure 3b). None of the existing formulations can capture the behaviour of the φ_h observed in the present data set. Notice that φ_h is directly proportional to $\partial\theta/\partial z$ and inversely proportional to θ_*. The variation of φ_h with respect to $\partial\theta/\partial z$ and θ_* has been analysed separately to find the possible cause of the large scattering in φ_h (data not shown). It is observed that the scatter in φ_h, which occurs in the case of near-neutral conditions as well as other stability regimes with a relatively large φ_h, is better correlated with the scatter in $\partial\theta/\partial z$. In the intermediate range for φ_h, both $\partial\theta/\partial z$ and θ_* appear to be equally responsible for the scatter in φ_h, while for a smaller φ_h, θ_* appears to be the dominant factor in the scattering in φ_h. Owing to the large scatter and associated uncertainty in the estimation of φ_h in the near-neutral condition, it is not obvious to propose a functional form of φ_h for a full range of ζ for this data set. However, for consistency with the functional form of φ_m suggested above, it is recommend to use the function φ_h proposed by Grachev *et al.* (2007a) in its existing form for application purposes over the Indian region.

One can speculate that a functional dependency of φ_m on stability parameter ζ might be associated with the self-correlation due to the shared variables u_* and θ_* in both the dependent ($\varphi_{m,h}$) and independent (ζ) variables. To overcome the impact of spurious correlation on the analysis of the functional forms of φ_m and φ_h with ζ, the methodology suggested by Grachev *et al.* (2013) in which the shared variable is replaced by another universal function was adopted. In the analysis of φ_m with ζ, friction velocity u_* comes as a common variable which is replaced using another universal functional form of the normalized standard deviation of the vertical wind velocity fluctuation σ_w as $\sigma_w/u_* = \varphi_w$. This leads to:

$$\frac{kz}{\sigma_w}\frac{\partial U}{\partial z} = \varphi_m \varphi_w{}^{-1}.$$

Similarly for φ_h:

$$\frac{kz}{\sigma_\theta}\frac{\partial \theta}{\partial z} = \varphi_h \varphi_\theta{}^{-1},$$

where σ_θ is the standard deviation of the temperature fluctuations; and φ_θ is the corresponding stability-dependent functional form. The problem of self-correlation can be overcome in such a hybrid representation of φ_m and φ_h. Babić *et al.* (2016) have found that an increase in $\varphi_m \varphi_w^{-1}$ is slower than that predicted by the linear functional form of φ_m. Thus, the analysis presented by Babić *et al.* suggests that a relatively slow rate in the increase of φ_m is not caused by self-correlation.

Figure 2c shows the variation of $\left(\frac{kz}{\sigma_w}\right)\frac{\partial U}{\partial z}$ with ζ in which the dotted green line represents $\varphi_m \varphi_w{}^{-1}$ with $\varphi_m = 1 + \beta_m \zeta$ (Businger *et al.*, 1971) and $\varphi_w = 1.25\,(1 + 0.2\zeta)$ (Kaimal and Finnigan, 1994). The continuous blue line represents $\varphi_m \varphi_w{}^{-1}$ with $\varphi_m(\zeta) = 1 + \frac{5.4\zeta(1+\zeta)^{\frac{1}{3}}}{1+0.89\zeta}$, (Grachev *et al.*, 2007a) and $\varphi_w = 1.21(1 + 1.34\zeta)^{1/3}$, which is the best-fit curve for the present filtered data set. Similarly, Figure 3c shows the variation of $\left(\frac{kz}{\sigma_\theta}\right)\frac{\partial \theta}{\partial z}$ with ζ in which the dotted green line represents $\varphi_h \varphi_\theta{}^{-1}$ with $\varphi_h = 1 + \beta_h \zeta$ (Businger *et al.*, 1971) and $\varphi_\theta = 2.0\,(1 + 0.5\zeta)^{-1}$ (Kaimal and Finnigan, 1994). The continuous blue line represents $\varphi_h \varphi_\theta{}^{-1}$ with $\varphi_h(\zeta) = 1 + \frac{5\zeta + 5\zeta^2}{1 + 3\zeta + \zeta^2}$, (Grachev *et al.*, 2007a) and $\varphi_\theta = 18.0(1 + 28.1\zeta)^{-0.5}$; it is the best-fit curve for the present filtered data set. In the case of normalized wind shear (Figure 2c), no substantial changes are observed in the amount of scattering as compared with that observed for the φ_m *versus* ζ plot (Figure 2a), suggesting that the proposed formulation of φ_m is not affected by self-correlation. This is consistent with the findings of Babić *et al.* (2016) and Grachev *et al.* (2018). Further, the combination of the functional form of φ_m and φ_w suggested here can capture the observed functional dependence of $\left(\frac{kz}{\sigma_w}\right)\frac{\partial U}{\partial z}$ with ζ. However, in the case of the temperature gradient, a relatively smaller scatter is observed in the plot of $\left(\frac{kz}{\sigma_\theta}\right)\frac{\partial \theta}{\partial z}$ with ζ (Figure 3c) in near-neutral conditions as compared with that observed in φ_h vs ζ plot (Figure 3a), indicating a possible presence of spurious correlation between the φ_h and ζ relationship,

specifically in near-neutral conditions. In addition, the combination of the functional forms of φ_h and φ_θ suggested here fails to capture the observed functional dependence of $\left(\frac{kz}{\sigma_\theta}\right)\frac{\partial\theta}{\partial z}$ with ζ in a quantitative manner. This can be attributed to the fact that both the functional forms of φ_h and φ_θ (plot not shown) show a relatively weak dependence on stability parameter ζ.

5 | CONCLUSIONS

Turbulence observations over an Indian region are used for the analysis of observational-based functional forms of stability-correction functions for momentum (φ_m) and heat (φ_h) commonly used for the estimation of surface fluxes in atmospheric models. The approach of Grachev *et al.* (2013) is followed to filter out the cases in which the Monin–Obukhov similarity theory (MOST) is, in general, assumed to be invalid. The filtered observational data suggest that the stability-correction function for momentum increases with a relatively slow rate as compared with that shown by the classical linear form in the range $0.5 < \zeta < 1$. Further, the observed φ_m are found to be relatively small for $0.5 < \zeta < 2$ as compared with those predicted by the functional form suggested by Cheng and Brutsaert (2005). It does not show a levelling-off characteristic as suggested by Cheng and Brutsaert (2005) and supports the arguments of Grachev *et al.* (2007a) and Babić *et al.* (2016). The functional form of φ_m suggested by Grachev *et al.* (2007a) with optimized unknown parameters based on the present data set is relatively more appropriate. The functional form of φ_m over the region is given by:

$$\varphi_m(\zeta) = 1 + \frac{a_m\zeta(1+\zeta)^{\frac{1}{3}}}{1+b_m\zeta},$$

where $a_m = 5.4$ and $b_m = 0.89$. A relatively large scatter with an unexpectedly high φ_h in near-neutral conditions is observed, leading to uncertainty in the development of the functional form of φ_h function. Owing to an increased level of observed uncertainty involved in φ_h, it is perhaps better to use the functional form suggested by Grachev *et al.* (2007a) in its existing form. The modified form of φ_m along with the existing form of φ_h suggested by Grachev *et al.* can be used to estimate surface fluxes over an Indian region in numerical models of the atmosphere. Note that the validity of the proposed formulations is strictly dependent upon the applicability of the MOST because the concept that "universal stability-correction functions" exist in the atmospheric surface layer (ASL) holds good only in the regime in which the MOST is valid. It is still an open issue to parameterize correctly the turbulent fluxes beyond the range of applicability of the classical MOST.

ACKNOWLEDGEMENTS

The raw turbulence data for the Ranchi (India) site used in the present study can be obtained from the Indian National Centre for Ocean Information Service upon request (http://www.incois.gov.in/portal/datainfo/ctczdata.jsp). The work was partially supported by a J. C. Bose Fellowship to M. S. from Department of Science and Technology (DST)-Science and Engineering Research Board (SERB), Government of India (grant number SB/S2/JCB-79/2014). The authors thank the reviewers for comments and suggestions.

ORCID

Piyush Srivastava https://orcid.org/0000-0001-5379-5546
Maithili Sharan https://orcid.org/0000-0002-1893-8377

REFERENCES

Aditi and Sharan, M. (2007) Analysis of weak wind stable conditions from the observations of the land surface processes experiment at Anand in India. *Pure and Applied Geophysics*, 164, 1811–1837.

Arya, S.P. (1988) *Introduction to Micrometeorology*. San Diego, CA: Academic Press, p. 307.

Babić, K., Rotach, M.W. and Klaić, Z.B. (2016) Evaluation of local similarity theory in the wintertime nocturnal boundary layer over heterogeneous surface. *Agricultural and Forest Meteorology*, 228–229, 164–179.

Beljaars, A.C.M. and Holtslag, A.A.M. (1991) Flux parameterization over land surfaces for atmospheric models. *Journal of Applied Meteorology*, 30, 327–341.

Bhat, G.S. and Narasimha, R. (2007) Indian summer monsoon experiments. *Current Science*, 93, 153–164.

Brutsaert, W. (1982) *Evaporation into the atmosphere: Theory, history, and applications*. Dordrecht, Holland: Reidel Co, p. 299.

Businger, J.A., Wyngaard, J.C., Izumi, Y. and Bradley, E.F. (1971) Flux profile relationships in the atmospheric surface layer. *Journal of the Atmospheric Sciences*, 28, 181–189.

Cheng, Y.G. and Brutsaert, W. (2005) Flux–profile relationships for wind speed and temperature in the stable atmospheric boundary layer. *Boundary-Layer Meteorology*, 114, 519–538.

Clarke, R.H. (1970) Observational studies in the atmospheric boundary layer. *Quarterly Journal of the Royal Meteorological Society*, 96, 91–114.

Dwivedi, A.K., Chandra, S., Kumar, M., Kumar, S. and Kumar, N. V.P.K. (2014) Spectral analysis of wind and temperature components during lightning in pre-monsoon season over Ranchi. *Meteorology and Atmospheric Physics*, 127, 95–105.

Foken, T. (2006) 50 years of the Monin–Obukhov similarity theory. *Boundary-Layer Meteorology*, 119, 431–447.

Garratt, J.R. (1994) *The Atmospheric Boundary Layer. Cambridge Atmospheric and Space Science Series*. Cambridge, UK: Cambridge University Press, p. 336.

Grachev, A.A., Andreas, E.L., Fairall, C.W., Guest, P.S. and Persson, P.O.G. (2007a) SHEBA: flux–profile relationships in

stable atmospheric boundary layer. *Boundary-Layer Meteorology*, 124, 315–333.

Grachev, A.A., Andreas, E.L., Fairall, C.W., Guest, P.S. and Persson, P.O.G. (2007b) On the turbulent Prandtl number in the stable atmospheric boundary layer. *Boundary-Layer Meteorology*, 125, 329–341.

Grachev, A.A., Andreas, E.L., Fairall, C.W., Guest, P.S. and Persson, P.O.G. (2013) The critical Richardson number and limits of applicability of local similarity theory in the stable boundary layer. *Boundary-Layer Meteorology*, 147, 51–82.

Grachev, A.A., Fairall, C.W., Persson, P.O.G., Andreas, E.L. and Guest, P.S. (2005) Stable boundary-layer scaling regimes: the SHEBA data. *Boundary-Layer Meteorology*, 116, 201–235.

Grachev, A.A., Leo, L.S., Fernando, H.J.S., Fairall, C.W., Creegan, E., Blomquist, B.W., Christman, A.J., Hocut, C.M. (2018) Air-sea/land interaction in the coastal zone. *Boundary-Layer Meteorol*, 167, 181–210.

Grell, G.A., Dudhia, J., Stauffer, D.R. (1994) *A description of the fifth generation Penn State/NCAR mesoscale model (MM5). NCAR Technical Note NCAR/TN-398+STR*, p. 138.

Gryanik, V.M. and Lupkes, C. (2018) An efficient non-iterative bulk parametrization of surface fluxes for stable atmospheric conditions over polar sea-ice. *Boundary-Layer Meteorology*, 166, 301–325.

Hicks, B.B. (1976) A note on the log-linear velocity profile in stable conditions. *Quarterly Journal of the Royal Meteorological Society*, 102, 703–707.

Holtslag, A.A.M. and De Bruin, H.A.R. (1988) Applied modeling of the nighttime surface energy balance over land. *Journal of Applied Meteorology*, 27, 689–704.

Jimenez, P.A., Dudhia, J., Gonzalez-Rouco, J.F., Navarro, J., Montavez, J.P. and Gracia-Bustamante, E. (2012) A revised scheme for the WRF surface layer formulation. *Monthly Weather Review*, 140, 898–918.

Kaimal, J.C. and Finnigan, J.J. (1994) *Atmospheric Boundary Layer Flows: Their Structure and Measurements*. Oxford: Oxford University Press.

Krishnan, P. and Kunhikrishnan, P.K. (2002) Some Characteristics of Atmospheric Surface Layer over a Tropical Inland Region during SouthwestMonsoon Period. *Atmospheric Research*, 62, 11–124.

Li, D. (2019) Turbulent Prandtl number in the atmospheric boundary layer—where are we now? *Atmospheric Research*, 216, 86–105.

Luhar, A.K., Hurley, P.J. and Rayner, K.N. (2009) Modelling near-surface low winds over land under stable conditions: sensitivity tests, flux–gradient relationships, and stability parameters. *Boundary-Layer Meteorology*, 130(2), 249–274.

Mahrt, L. (1998) Stratified atmospheric boundary layers and breakdown of models. *Theoretical and Computational Fluid Dynamics*, 11, 263–279.

Monin, A.S. and Obukhov, A.M. (1954) Osnovnye zakonomernosti turbulentnogo peremeshivanija v prizemnom sloe atmosfery (basic laws of turbulent mixing in the atmosphere near the ground). *Trudy geofiz. Inst. AN SSSR*, 24(151), 163–187.

Park, S.-J., Park, S.-U., Ho, C.-H. and Mahrt, L. (2009) Flux–gradient relationship of water vapor in the surface layer obtained from CASES-99 experiment. *Journal of Geophysical Research*, 114, D08115.

Patil, M.N. (2006) Aerodynamic drag co-efficient and roughness length for three seasons over a tropical western Indian station. *Atmospheric Research*, 80, 280–293.

Pielke, R. (2013) *Mesoscale Meteorological Modeling*. New York: Academic Press, p. 760.

Ramachandran, R., Prakash, J.W.J., Sen Gupta, K., Nair, K.N. and Kunhikrishnan, P.K. (1994) Variability of surface roughness and turbulence intensities at a coastal site in India. *Boundary-Layer Meteorology*, 70, 385–400.

Ramana, M.V., Krishnan, P. and Kunhikrishnan, P.K. (2004) Surface boundary layer characteristics over a tropical inland station: seasonal features. *Boundary-Layer Meteorology*, 111, 153–175.

Rao, K.G. and Narasimha, R. (2006) Heat–flux scaling for weakly forced turbulent convection in atmosphere. *Journal of Fluid Mechanics*, 547, 115–135.

Rao, K.G., Narasimha, R. and Prabhu, A. (1996) Estimation of drag coefficient at low wind speeds over the monsoon trough land region during MONTBLEX-90. *Geophysical Research Letters*, 23, 2617–2620.

Rao, K.G. and Reddy, N.N. (2019) On moisture flux of the Indian summer monsoon: a new perspective. *Geophysical Research Letters*, 46, 1794–1804. https://doi.org/10.1029/2018GL080392.

Reddy, N.N. and Rao, K.G. (2016) Roughness lengths at four stations within the micrometeorological network over the Indian monsoon region. *Boundary-Layer Meteorology*, 158, 151–164.

Sharan, M. and Kumar, P. (2011) Estimation of upper bounds for the applicability of nonlinear similarity functions for non-dimensional wind and temperature profiles in the surface layer in very stable conditions. *Proceedings of the Royal Society A*, 467, 473–494.

Sharan, M. and Srivastava, P. (2016) Characteristics of heat flux in the unstable atmospheric surface layer. *Journal of the Atmospheric Sciences*, 73, 4519–4529.

Skamarock, W.C., Klemp, J.B., Dudhia, J., Gill, D.O., Barker, D.M., Duda, M.G., Huang, X., Wang, W. and Powers, J.G. (2008) *A description of the advanced research WRF Version 3*. Technical Report: TN-475+STR, NCAR, p. 133.

Srivastava, P. and Sharan, M. (2015) Characteristics of drag coefficient over a tropical environment in convective conditions. *Journal of the Atmospheric Sciences*, 72, 4903–4913.

Srivastava, P. and Sharan, M. (2019) Analysis of dual nature of heat flux predicted by Monin–Obukhov similarity theory: an impact of empirical forms of stability correction functions. *Journal of Geophysical Research*, 124, 3627–3646. https://doi.org/10.1029/2018JD029740.

Stull, R. (1988) *An Introduction to Boundary Layer Meteorology*, Kluwer Academic Publishers, Netherlands, p. 666.

Tyagi, B., Satyanarayana, A.N.V., Kumar, M. and Mahanti, N.C. (2012) Surface energy and radiation budget over a tropical station: an observational study. *Asia-Pacific Journal of Atmospheric Sciences*, 48, 411–421.

Webb, E.K. (1970) Profile relationships: the log-linear range and extension to strong stability. *Quarterly Journal of the Royal Meteorological Society*, 96, 67–90.

Wyngaard, J.C. (2010) *Turbulence in the Atmosphere*. New York, NY: Cambridge University Press.

Yagüe, C., Viana, S., Maqueda, G. and Redondo, J. (2006) Influence of stability on the flux–profile relationships for wind speed, ϕ_m, and temperature, ϕ_h, for the stable atmospheric boundary layer. *Nonlinear Processes in Geophysics*, 13, 185–203.

Zhang, J.A., Nolan, D.S., Rogers, R.F. and Tallapragada, V. (2015) Evaluating the impact of improvements in the boundary layer parameterizations on hurricane intensity and structure forecasts in HWRF. *Monthly Weather Review*, 143, 3136–3315.

How to cite this article: Srivastava P, Sharan M, Kumar M, Dhuria AK. On stability correction functions over the Indian region under stable conditions. *Meteorol Appl*. 2020;27:e1880. https://doi.org/10.1002/met.1880